Signal Processing 92 (2012) 357–362

Contents lists available at ScienceDirect

Signal Processing

journal homepage: www.elsevier.com/locate/sigpro

Compressed sensing of complex-valued data

Siwei Yu [a], A. Shaharyar Khwaja [a], Jianwei Ma [b,c,*]

[a] School of Aerospace, Tsinghua University, Beijing 100084, China
[b] Department of Mathematics, Florida State University, Tallahassee, FL 32306, USA
[c] Institute of Applied Mathematics, Harbin Institute of Technology, Harbin 15001, China

ARTICLE INFO

Article history:
Received 31 May 2011
Received in revised form
23 July 2011
Accepted 28 July 2011
Available online 10 August 2011

Keywords:
Compressed sensing
Image reconstruction
Terahertz imaging

ABSTRACT

Compressed sensing (CS) is a recently proposed technique that allows the reconstruction of a signal sampled in violation of the traditional Nyquist criterion. It has immediate applications in reduction of acquisition time for measurements, simplification of hardware, reduction of memory space required for data storage, etc. CS has been applied usually by considering real-valued data. However, complex-valued data are very common in practice, such as terahertz (THz) imaging, synthetic aperture radar and sonar, holography, etc. In such cases CS is applied by decoupling real and imaginary parts or using amplitude constraints. Recently, it was shown in the literature that the quality of reconstruction for THz imaging can be improved by applying smoothness constraint on phase as well as amplitude. In this paper, we propose a general l_p minimization recovery algorithm for CS, which can deal with complex data and smooth the amplitude and phase of the data at the same time as well has the additional feature of using a separate sparsity promoting basis such as wavelets. Thus, objects can be better detected from limited noisy measurements, which are useful for surveillance systems.

1. Introduction

In many engineering fields such as geophysical exploration, magnetic resonance imaging (MRI) and remote sensing, we have to deal with the problem of incomplete and inaccurate measurements arising due to physical constraints or extremely expensive data acquisition equipment. Compressed sensing (CS) is a technique used for encoding large-scale sparse signals using a relatively small number of linear measurements, and minimizing the l_1 norm in order to reconstruct/decode the signal. It has been explored and presented in a number of references, especially [1–5] that present the theory and applications of CS, e.g. data compression, channel coding, inverse problems, data acquisition, single-pixel imaging, etc.

Traditionally, CS has been used with real data. However, complex-valued data are very common in practical situations, such as terahertz (THz) imaging [6,7], synthetic aperture radar (SAR) [8] and sonar (SAS) [9], MRI [10], etc. where a 2D complex image of the observed object is obtained and the phase of the complex image can provide extra information about the properties of the object. Therefore, it is useful to devise CS-based algorithms that can deal with such type of images. It was shown in [11] that the problem of CS reconstruction for complex-valued data can be easily modified by arranging the real and imaginary parts of the data in a single real-valued array and applying CS to this array. However, one disadvantage of the method pointed out in [11] is that the real and imaginary parts of the observed signal are decoupled and thus any prior phase information is not exploited. This prior information may be the smoothness of original data in phase and amplitude that after acquisition appears to be rough or noisy, or the presence of discontinuities in both amplitude and phase. Ref. [12] proposed a method for feature-preserving of complex-valued SAR imaging where amplitude constraints were used as prior

* Corresponding author at: Department of Mathematics, Florida State University, Tallahassee, FL 32306, USA. Tel.: +1 850 559 6085; fax: +1 850 645 9166.
E-mail addresses: jma2@fsu.edu, jma@hit.edu.cn (J. Ma).

0165-1684/$ - see front matter © 2011 Elsevier B.V. All rights reserved.
doi:10.1016/j.sigpro.2011.07.022

knowledge for enhancing point scatterers as well as reducing speckle noise. The work in [13] and [14] presents sparse reconstruction of complex signals in CS THz imaging and hyperspectral imaging. This technique suggests a smoothing constraint on the phase of the signal and uses a sparse transform for the data. It has been shown that the reconstruction quality is improved by using smoothing constraints for phase as well as amplitude, compared to the case where phase information is not exploited. We present an extension of the approach in [13] by proposing a method to put constraints on both amplitude and phase of the data, besides using a separate sparse transform for the data such as the wavelet transform. This method is based on Newton's method as used in [12] and can be used for l_p minimization, where $0<p<1$. The method presented in this paper can be applied to THz imaging to reduce the number of required measurements as well as improve signal-to-noise ratio (SNR). This is useful as reducing acquisition time is one of the major concerns towards achieving real-time THz imaging and traditional rapid acquisition techniques result in a loss of SNR [15]. We would like to point out here that whereas complex-valued data can be handled by the implementations provided by [16–19], our purpose is not only to use complex-valued data in CS-based recovery, but also to take into account any relationship between amplitude and phase of such type of data that can help in reconstruction process based on a general l_p-norm minimization.

2. Basics of compressed sensing

Let $f \in C^N$ be a complex signal that is sampled. It has a sparse representation over a transform Ψ. This means we have a coefficient vector x such that $x=\Psi f$ with $\|x\|_0 = K \ll N$, where $\|x\|_0$ stands for the number of nonzero elements in x. We call f a K-sparse signal over the transform Ψ. Similarly, let $\Phi \in R^{M\times N}(M<N)$ be the measurement matrix. Using Φ, we obtain the measured signal g, which is a linear combination of the elements of f. The length of g is M, which means we have fewer measurements than the degrees of freedom of signal f. Based on this discussion, we can write the signal model as follows:

$$g=\Phi f+\xi \tag{1}$$

or

$$g=\Phi\Psi^{-1}x+\xi, \quad f=\Psi^{-1}x \tag{2}$$

where ξ denotes possible measurement noise, and Ψ^{-1} denotes inverse transform of Ψ. Eq. (1) or (2) is an ill-conditioned underdetermined problem and one cannot solve it directly to recover f. However, if Φ satisfies a property known as the restricted isometric property (RIP) [1,4], f can be recovered by solving an l_1 minimization or basis pursuit problem [1] given as follows:

$$\hat{f}=\arg\min_f J(f),$$

$$J(f)=\|g-\Phi f\|_2^2+\lambda_1\|\Psi f\|_1. \tag{3}$$

In [20], it is further shown that when it may not be possible to recover f, Ψf can still be recovered using (3) if a property known as D-RIP is satisfied. The first term in (3) represents the closeness of the solution to the observations, while the second term represents a priori information about sparsity. Usually Φ is chosen as a random matrix, such as Gaussian or ± 1 binary entries inside, which can satisfy the RIP or D-RIP properties. Eq. (3) can be solved using different recovery methods given in [1,16–19,21], etc. It has also been shown in [22] that a variant of basis pursuit can reconstruct f using fewer measurements. In this variant, l_1 minimization is replaced by a general l_p minimization. The objective function is described as

$$J(f)=\|g-\Phi f\|_2^2+\lambda_1\|\Psi f\|_p^p, \tag{4}$$

with $0<p<1$.

3. CS for complex-valued data

The complex-valued data f can be expressed as $f=|f|e^{jP}$, where P is the phase and $|f|$ is the magnitude of the complex-valued data f. The matrices Φ, g and f can be transformed to correspond to the case of real data as shown in [11]. However, in this case the real and imaginary parts are decoupled and we do not make use of any prior information about the complex data. A modification is proposed in [23] to incorporate phase information by rewriting the objective function in (3) as follows to take into account complex signals:

$$J(f)=\|g-\Phi e^{jP}|f|\|_2^2+\lambda_1\|\Psi|f|\|_1. \tag{5}$$

This method is used to compensate for phase errors arising due to acquisition equipment in MRI. Ref. [12] puts constraints on the amplitude of the complex data in order to obtain point and region-based feature enhanced imaging for the case of SAR data. Although the method in [12] is presented as a SAR imaging method, it can be applied in CS scenarios. The method is based on the optimization of following objective function:

$$J(f)=\|g-\Phi f\|_2^2+\lambda_1\||f|\|_p^p+\lambda_2\|D|f|\|_p^p, \tag{6}$$

where D represents a two-dimensional (2D) gradient operator. This equation is used for enhancing point scatterers as well as reducing speckle. Ref. [24] uses similar idea as presented in [23] for feature enhancing in case of SAR data acquired with unknown sensor motion errors. Ref. [13] goes one step further and shows that quality of reconstructed signal can be improved by using additional prior information about the phase as follows:

$$J(f)=\|g-\Phi f\|_2^2+\lambda_1\|\Psi f\|_1+\lambda_2\|P-\overline{P}\|_2^2. \tag{7}$$

In this case a sparse transform can be used and the phase can be smoothed as well. P represents the phase of f and $\overline{P}$ is the average of the phase in the neighborhood of a pixel. Here, the third term means that the phase of the reconstructed signal varies smoothly with respect to its neighboring pixels.

We propose to provide extra features of sparse transforms, amplitude and phase smoothing using a general l_p minimization. This problem can be expressed as

$$\hat{f}=\arg\min_f J(f),$$

$$J(f) = \|g - \Phi f\|_2^2 + \lambda_1 \|\Psi |f|\|_p^p + \lambda_2 \|D|f|\|_p^p + \lambda_3 \|DP\|_p^p. \quad (8)$$

The 2D derivative operator D is given as

$$D = \sqrt{D_x^2 + D_y^2}, \quad (9)$$

where D_x and D_y represent the gradients in horizontal and vertical directions, respectively. The first term on the right side of (8) is a data fidelity term, which means the solution we get is close to our observations. The other terms contain some prior information to promote sparsity. The second term promotes sparsity over transform Ψ, the third and last terms promote sparsity of the gradient of the amplitude and phase, which can help us reduce noise. The use of the derivative operator also helps in preserving discontinuities. The phase smoothing has been shown to improve performance in the case of THz and hyperspectral imaging in [13] and [14] as well as interferometric SAR in [25].

We extend the method proposed in [12] to solve (8). This method can take into account complex-valued data and different values of p, and is also described as convergent. The main steps involved in the solution are given as follows:

1. In order to avoid problems due to non-differentiability of the l_p-norm around the origin, we will use the following smooth approximation to the l_p-norm in (8) [12]:

$$\|f\|_p^p \approx \sum_{i=1}^{N} (|(f)_i|^2 + \varepsilon)^{p/2}, \quad (10)$$

where $\varepsilon > 0$ is a small constant and (f_i) is the ith element of f.

2. Subsequently, we can write the objective function in (8) as follows:

$$J(f) = \|g - \Phi f\|_2^2 + \lambda_1 \sum_{i=1}^{N} (|(\Psi |f|)_i|^2 + \varepsilon)^{p/2} + \lambda_2 \sum_{i=1}^{N} (|(D|f|)_i|^2 + \varepsilon)^{p/2} + \lambda_3 \sum_{i=1}^{N} (|(DP)_i|^2 + \varepsilon)^{p/2}. \quad (11)$$

3. To minimize (11), we use quasi-Newton method with a new Hessian update scheme as proposed in [12]. We

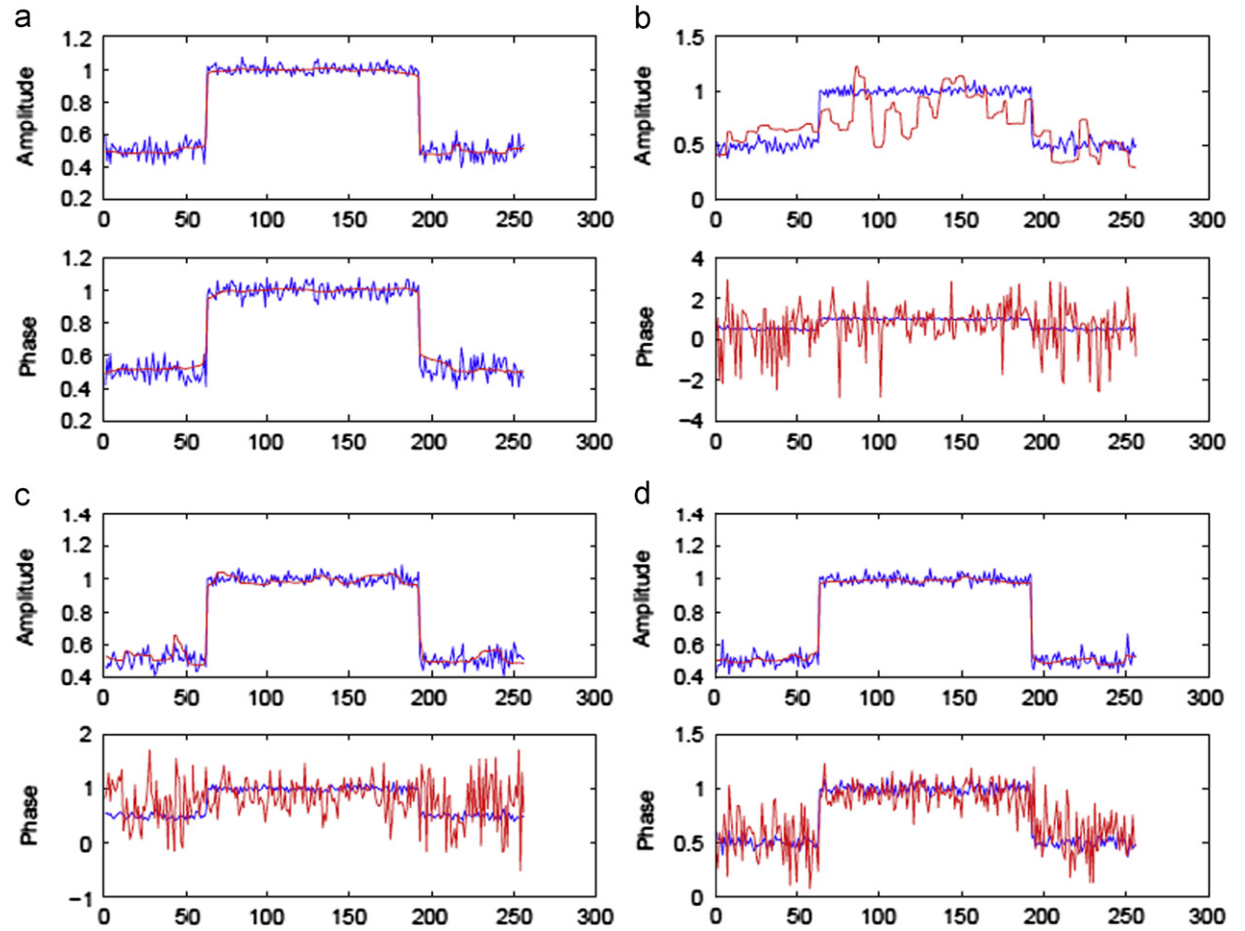

Fig. 1. Amplitude and phase of reconstructed "Complex" 1D data (red Line). (a) Using 50% measurements and $\lambda_1 = 0.054, \lambda_2 = 0.114, \lambda_3 = 0.240$; SNR of reconstructed data = 28 dB. (b)–(d) Using parameters $\lambda_1 = 0.054, \lambda_2 = 0.114, \lambda_3 = 0$. (b) Using 50% measurements; SNR of reconstructed data = 1 dB. (c) 60% measurements; SNR = 9 dB. (d) 80% measurements; SNR = 15 dB. (For interpretation of the references to color in this figure legend, the reader is referred to the web version of this article.)

first have to take gradient of $J_m(f)$ with respect to real and imaginary parts of f and arrange the result in a compact form of $\nabla J(f)=2(\partial J/\partial \bar{f})$ given as follows:

$$\nabla J(f)=\tilde{H}(f)f-2\Phi^H g+\Lambda_{33}, \tag{12}$$

where

$$\tilde{H}(f)=2\Phi^H\Phi+\lambda_1 p\Phi^H\Psi^{-1}\Lambda_1\Phi\Psi+\lambda_2 p\phi^H D^T\Lambda_2 D\phi,$$

$$\Lambda_1(f)=\mathrm{diag}\{((\Psi|f|)_i^2+\varepsilon)^{p/2-1}\},$$

$$\Lambda_2(f)=\mathrm{diag}\{((D|f|)_i^2+\varepsilon)^{p/2-1}\},$$

$$\Lambda_3(f)=\mathrm{diag}\{(DP)_i^2+\varepsilon)^{p/2-1}\},$$

$$\Lambda_{33}(f)=\frac{\lambda_3 p}{j}XD^T\Lambda_3 DP,$$

$$X=\mathrm{diag}\{-1/(\bar{f}_n)\},$$

$$P=\angle f=\frac{1}{2j}\ln\frac{f}{\bar{f}},$$

$$\Phi(f)=\mathrm{diag}\{e^{-j\phi[(f)_i]}\}. \tag{13}$$

Here $\phi[(f)_i]$ denotes the phase of the complex number $(f)_i$, $(\cdot)^H$ denotes the Hermitian of a matrix and diag is a diagonal matrix whose ith diagonal element is given by the expression inside the brackets. $\bar{f}$ denotes the complex conjugate of f, and j refers to $\sqrt{-1}$.

4. The gradient calculated in the previous step is used in the following quasi-Newton iteration:

$$(\hat{f})^{(n+1)}=(\hat{f})^n-\gamma[\tilde{H}((\hat{f})^n)]^{-1}\nabla J((\hat{f})^n), \tag{14}$$

where γ is the step size. After substituting (12) into (14) and rearranging, we obtain our iterative algorithm

$$\tilde{H}((\hat{f})^n)(\hat{f})^{(n+1)}=(1-\gamma)\tilde{H}((\hat{f})^n)(\hat{f})^n+2\gamma\Phi^H g-\gamma\Lambda_{33}. \tag{15}$$

We stop our iteration when $\|(\hat{f})^{(n+1)}-(\hat{f})^n\|_2^2/\|(\hat{f})^n\|_2^2<\delta$, where δ is a small constant.

4. Simulation results

In this section, we apply the technique presented in this paper to both 1D and 2D simulated data as well as THz data. We show that in case of a complex signal having originally smooth amplitude or phase as well as similar amplitude and phase discontinuities such as in THz data, we can apply the technique to not only reconstruct the signal from CS measurements, but also denoise the data simultaneously. Reconstructed image quality is judged visually as well as by calculating SNR of reconstructed signal with respect to the original noiseless signal. The values of p and γ are fixed at 0.9 and 0.8, respectively for all the results. The values of λ_1, λ_2 and λ_3 are chosen by trial-and-error to maximize the SNR. ε is a small number, e.g.,

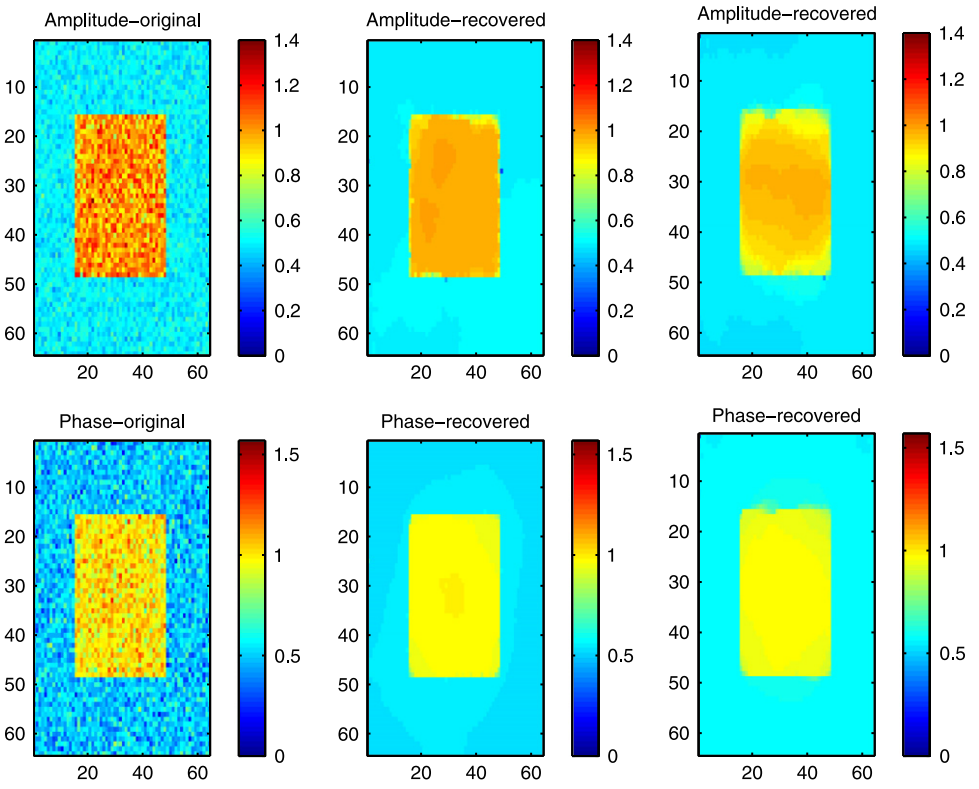

Fig. 2. Amplitude and phase of reconstructed "Complex" 2D data using 25% measurements. (left) Original data. (middle) Reconstruction by using parameters $\lambda_1=0,\lambda_2=0.114,\lambda_3=0.048$; SNR=17 dB. (right) Reconstruction by using parameters $\lambda_1=0.054,\lambda_2=0.114,\lambda_3=0.048$; SNR=20 dB.

10^{-5} as used in [12] and [23]. For $p<1$, the optimization problem is non-convex, therefore, the solution obtained is sensitive to initial estimate. We use the initial estimate as $\Phi^H g$ and obtain reasonable reconstructions with this estimate. Firstly, a 1D signal that is a smooth step function in both amplitude and phase is considered and noise is added to it. The length of the signal is 256 pixels. The noisy signal is shown in Fig. 1 as the blue line. We multiply this signal with a random measurement matrix (the number of rows is half the number of columns) such that the number of samples is reduced by 50%. Reconstruction of the signal is shown in Fig. 1(a), along with the values of λ_1, λ_2 and λ_3. It can be observed that both amplitude and phase of the signal appear smooth in the reconstructed signal. In Fig. 1(b)–(d), we show comparisons of reconstructed results with parameter $\lambda_3=0$ (i.e., without phase constraint) using 50%, 60% and 80% measurements, respectively. The results indicate that in order to obtain the original signal without noise, a larger number of measurements are needed and even in case of 80% measurements, the recovered phase is not smooth as there is no such constraint for the phase. Thus, we can conclude that using a phase constraint allows us to reconstruct the original complex signal as well as denoise it using a lesser number of measurements. This may be due to the fact that by using phase constraints, we make use of more prior information about the signal and this can be useful for reducing image acquisition time.

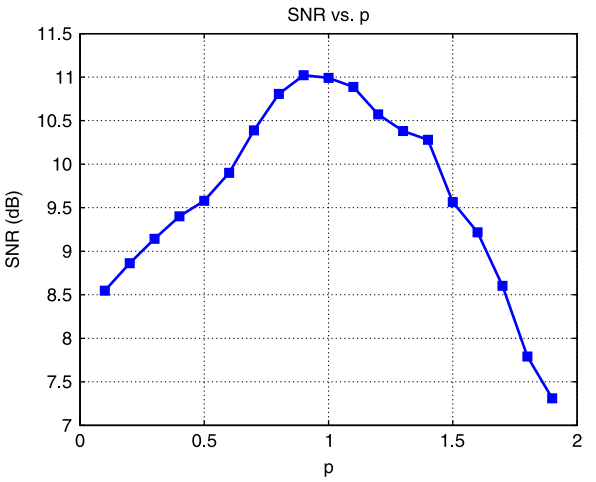

Fig. 3. SNR vs. p for THz data (the maximum occurs at $p=0.9$).

We also display results for a 64×64 2D simulated data consisting of a square with amplitude equal to 1 in the middle of a background having an amplitude equal to 0.5. The phase is $\pi/3$ rad for the square in the middle and $\pi/6$ rad elsewhere. We add a background noise to the data (see Fig. 2, left). Fig. 2 shows the reconstructed results using 25% measurements and different parameters. The proposed method leads to smooth amplitude and phase and a higher SNR, compared to the method where $\lambda_1=0$. We further carry out reconstruction using actual THz data used in [26]. About 50% measurements were used for the reconstruction. The corresponding graph of SNR versus different values of p in Fig. 3 shows

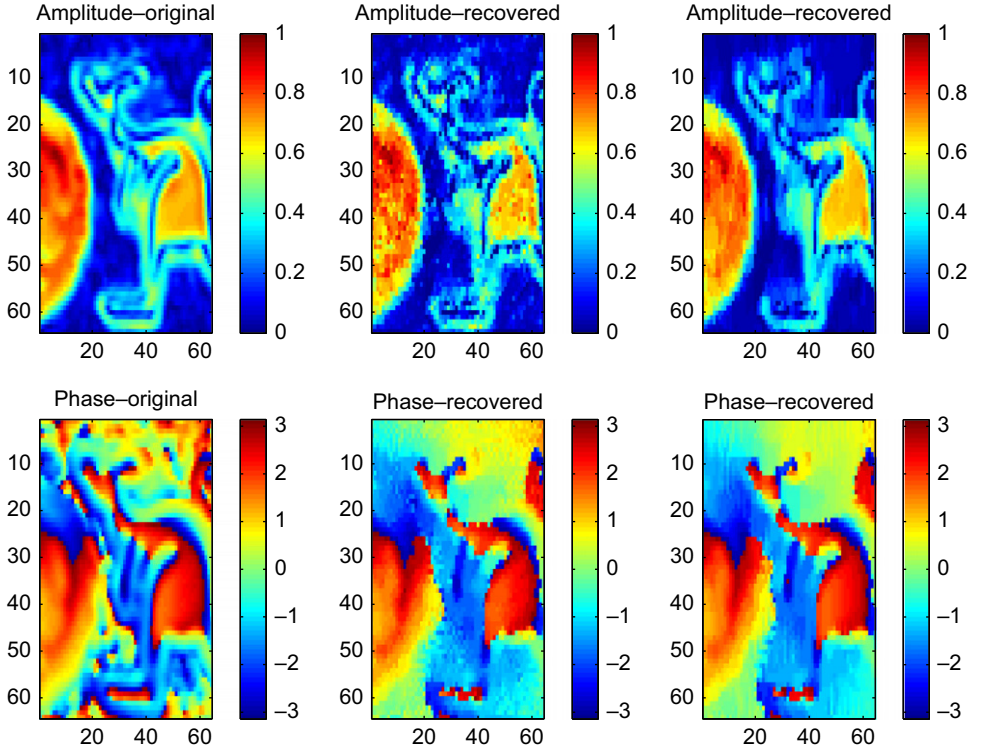

Fig. 4. Amplitude and phase of reconstructed THz data using 50% measurements. (left) Original data. (middle) Reconstruction by using $\lambda_1=0,\lambda_2=0.0114,\lambda_3=0.0048$; SNR=10 dB. (right) Reconstruction by using $\lambda_1=0.0054,\lambda_2=0.0114,\lambda_3=0.0048$; SNR=11 dB.

that the highest SNR is achieved at $p=0.9$. The values of p range from 0.1 to 2 in a step size of 0.1 are used to demonstrate clearly that the SNR reaches its maximum at $p=0.9$ and then decreases for greater values of p. As our method is based on a general l_p minimization instead of fixed l_1 minimization, we have more flexibility to choose a value for p that will give a better SNR. The time taken by non-optimized MATLAB code for the THz data reconstruction is 20 min, using a system with Intel Core 2 Duo Processor E8400 (3 GHz) and 4 GB RAM. Further results with $\lambda_1 = 0$ and a non-zero λ_1 are shown in the middle and right columns of Fig. 4, respectively for the THz data. It can be seen that in the latter case, the amplitude is better reconstructed, whereas the quality of the phase seems to be almost the same in both cases. Due to the complicated contour like nature of the data, the phase has various discontinuities that prevent the exact reconstruction of phase using only smoothness constraints, however, the advantage of using a non-zero λ_1 is demonstrated along with complex CS reconstruction that gives an amplitude and phase resembling the original smooth nature of the data. The results indicate that the feature of having an additional sparsity promoting basis helps in reconstructing the image with a better SNR. As comparison, we also carried out reconstruction using IST (iterative shrinkage/thresholding) [19], without using any phase constraint. The reconstructed data are then denoised using the total variation smoothing technique in [27]. We obtained SNRs of 18 dB and 15 dB for the simulated 1D and 2D data, and an SNR of 8 dB for the THz data. These SNRs further demonstrate that taking into account phase constraint for complex-valued data improves reconstruction performance.

5. Conclusion

In this paper, we present a general l_p-norm minimization that can handle both amplitude and phase smooth constraints for complex-valued data compressed sensing as well as a separate sparsity-promoting constraint at the same time. We show good performance of the method for both 1D data and 2D complex data containing noise. It has been demonstrated that using phase constraint allows us to reconstruct with less data and we can also use an additional sparsity promoting basis besides the smooth constraints that help to further improve the reconstructed image quality. The proposed technique can be applied for terahertz imaging and SAR. Further improvements in the phase reconstruction will be explored in future work. Some existing fast decoding methods from the community of CS can be also applied to our strategy of complex-valued CS.

Acknowledgment

The authors are grateful to Dr. Dan Popescu of CSIRO ICT Center, Australia, for providing the terahertz data used in [26]. We are also thankful to the reviewers for their comments that helped us improve our paper.

References

[1] E. Candès, E. Tao, Decoding by linear programming, IEEE Trans. Inf. Theory 51 (12) (2005) 4203–4215.
[2] E. Candès, J. Romberg, T. Tao, Robust uncertainty principles: exact signal reconstruction from highly incomplete frequency information, IEEE Trans. Inf. Theory 52 (2) (2006) 489–590.
[3] D. Donoho, Compressed sensing, IEEE Trans. Inf. Theory 52 (4) (2006) 1289–1306.
[4] E. Candès, E. Wakin, An introduction to compressive sampling, IEEE Signal Process. Mag. 25 (2) (2008) 21–30.
[5] R. Baraniuk, Compressed sensing, IEEE Signal Process. Mag. 24 (4) (2007) 14–20.
[6] D. Mittleman, Sensing with terahertz radiation, Springer Series in Optical Sciences 85 (2003).
[7] S. Luryi, J. Xu, A. Zaslavsky, Terahertz spectroscopy and imaging, Future Trends in Microelectronics: Up the Nano Creek 359–368 (2007).
[8] I. Cumming, F. Wong, Digital Processing of Synthetic Aperture Radar Data, Artech House, Norwood, MA, 2005.
[9] M. Hayes, P. Gough, Synthetic aperture sonar: a review of current status, IEEE J. Ocean. Eng. 34 (3) (2009) 207–224.
[10] A. Webb, Magnetic Resonance Imaging, Introduction to Biomedical Imaging, Wiley, IEEE Press, 2003, pp. 157–219.
[11] J. Ender, On compressive sensing applied to radar, Signal Process. 90 (5) (2010) 1402–1414.
[12] M. Cetin, W.C. Karl, Feature-enhanced synthetic aperture radar image formation based on nonquadratic regularization, IEEE Trans. Image Process. 10 (4) (2001) 623–631.
[13] Z. Xu, W.L. Chan, D.M. Mittleman, E.Y. Lam, Sparse reconstruction of complex signals in compressed sensing terahertz imaging, Signal Recovery and Synthesis, OSA Technical Digest, 2009, paper STuA4.
[14] Z. Xu, E.Y. Lam, Hyperspectral reconstruction in biomedical imaging using terahertz systems, in: IEEE International Symposium on Circuits and System, 2010.
[15] X.-C. Zhang, Terahertz wave imaging: horizons and hurdles, Phys. Med. Biol. 47 (2002) 3667–3677.
[16] S. Becker, J. Bobin, E. Candès, NESTA: a fast and accurate first-order method for sparse recovery, SIAM J. Imaging Sci. 4 (1) (2009) 1–39.
[17] S. Becker, E. Candès, M. Grant, Templates for convex cone problems with applications to sparse signal recovery, to appear in Mathematical Programming Computation.
[18] E. van der Berg, M. Friedlander, Probing the Parento frontier for basis pursuit solutions, SIAM J. Sci. Comput. 31 (2008) 890–912.
[19] M. Elad, M. Zibulevsky, L1-L2 optimization in signal and image processing, IEEE Signal Process. Mag. 27 (3) (2010) 76–88.
[20] E. Candès, Y. Eldar, D. Needell, P. Randall, Compressed sensing with coherent and redundant dictionaries, Appl. Comput. Harmonic Anal., 31(1), pp. 59–73.
[21] J. Tropp, A. Gilbert, Signal recovery from random measurements via orthogonal matching pursuit, IEEE Trans. Inf. Theory 53 (12) (2008) 4655–4666.
[22] R. Chartrand, Exact reconstruction of sparse signals via nonconvex minimization, IEEE Signal Process. Lett. 14 (2007) 707–710.
[23] M. Lustig, D. Donoho, J. Pauly, Sparse MRI: the application of compressed sensing for rapid MRI, Magn. Reson. Med. 58 (6) (2007) 1182–1195.
[24] N. Onhon, M. Cetin, A nonquadratic regularization-based technique for joint SAR imaging and model error correction, in: Proceedings of SPIE, vol. 7337, 2009.
[25] L. Denis, F. Tupin, J. Darbon, M. Sigelle, Joint regularization of phase and amplitude of InSAR data: application to 3D reconstruction, IEEE Trans. Geosci. Remote Sens. 47 (11) (2009) 3774–3785.
[26] D. Popescu, A. Hellicar, Point spread function estimation for a terahertz imaging system, EURASIP J. Adv. Signal Process. 575817 (2010).
[27] L. Rudin, S. Osher, E. Fatemi, Nonlinear total variation based noise removal algorithms, Physica D 60 (1992) 259–268.